ACS OMEGA

Open Access

http://pubs.acs.org/journal/acsodf

Article

Enhancing Aqueous Solubility and Anticancer Efficacy of Oligochitosan-Folate-Cisplatin Conjugates through Oleic Acid Grafting for Targeted Nanomedicine Development

M. Tamilarasi Muniandy, Chin Fei Chee,* Noorsaadah Abdul Rahman,* and Tin Wui Wong*

Cite This: *ACS Omega* 2025, 10, 2428−2441

Read Online

ACCESS | Metrics & More | Article Recommendations

ABSTRACT: Oligochitosan is an anticancer water-soluble biomaterial. Conjugating cisplatin (anticancer drug) and folic acid (targeting ligand) with oligochitosan reduces its aqueous solubility, thus requiring excessive drug dose to be biologically active and organic instead of aqueous processing into nanomedicine. Covalent grafting of oleic acid onto oligochitosan-folate-cisplatin conjugate is envisaged to promote aqueous solubility via reducing interchain interaction, but it is challenging where multiple functional moieties are covalently attached onto a short oligomer (<5 kDa). This study produced oligochitosan-oleate-folate-cisplatin conjugate dissolvable in aqueous media pH 3−7, which represents common processing pH in drug vehicle development and tumor microenvironmental pHs. Oligochitosan-oleate conjugation was effected through *O*-acylation to provide amino groups of oligochitosan for folate and cisplatin grafting. Oligochitosan-folate-cisplatin conjugate was poorly soluble in aqueous and organic media. A degree of oleic acid substitution (DS) < 10% conferred aqueous solubility beyond which became less soluble due to hydrophobicity rise. Oligochitosan-oleate-folate-cisplatin conjugate with 4.51 ± 0.32% DS, 8.50 ± 0.57% folate content, and 0.94 ± 0.80% cisplatin content was dissolvable in aqueous media pH 3.3−7, conferring processing safety with improved cancer cytotoxicity in the nanoparticulate form at the acidic tumor microenvironment.

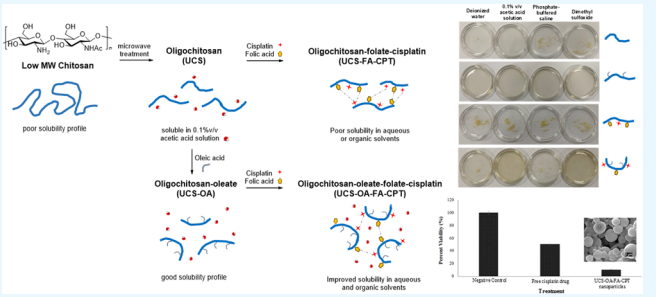

INTRODUCTION

Chitosan is a deacetylated derivative of chitin, the second most abundant polymer after cellulose.[1] It is a cationic polysaccharide constituting *N*-acetyl-D-glucosamine and D-glucosamine. Chitosan possesses amino and hydroxyl functional groups that enable chemical modification into covalent or complex derivatives for drug delivery applications.[2] *N*-trimethylated chitosan, a quaternary derivative of chitosan, has been developed to confer aqueous solubility and promote cellular uptake of therapeutics over a wide pH range due to its permanent ionic characteristics.[3−8] The ester forms of chitosan such as chitosan succinate, chitosan glutamate, and chitosan phthalate have been synthesized as matrix polymers for sustained drug release applications.[9]

Chitosan is available commercially in several grades: oligochitosan (<3.9 kDa), low molecular weight chitosan (<100 kDa), medium molecular weight chitosan (100−1000 kDa), and high molecular weight chitosan (>1000 kDa).[10] The aqueous solubility of chitosan is dictated by molecular weight and its solution pH, with smaller molecular weight chitosan and an acidic pH being favorable to promote its solubilization.[11−13] Chitosan is known to exert anticancer activity through raising the production of lymphokine and proliferation of cytotoxic T-lymphocytes.[14−17] Oligochitosan, the most soluble form of chitosan, has been reported to show a direct anticancer activity by interfering with cell metabolism, inhibiting cell growth and inducing apoptosis.[18] It is found to inhibit cancer growth by diminishing the metastasis colonies in vivo.[19−21] Higher molecular weight chitosans are however met with restricted use as they are poorly soluble in aqueous media.[16,20,22]

The latest cancer therapy has chitosan advances as the platform to develop drug delivery vehicles. Cancer therapeutics such as 5-fluorouracil,[23−26] doxorubicin,[27−29] gemcitabine,[30] methotrexate,[31,32] paclitaxel,[33,34] camptothecin,[35] daunorubicin,[36] 6-mercaptopurine,[37] docetaxel,[38,39] cisplatin,[40] and targeting ligands such as folate[41] and biotin[42] (vitamin), transferrin[38,43] (glycoprotein), trastuzumab[28] and cetuximab[44] (monoclonal antibody), estrone[45] (hormone), cyclic RGD

Received: April 12, 2024
Revised: October 23, 2024
Accepted: October 29, 2024
Published: January 17, 2025

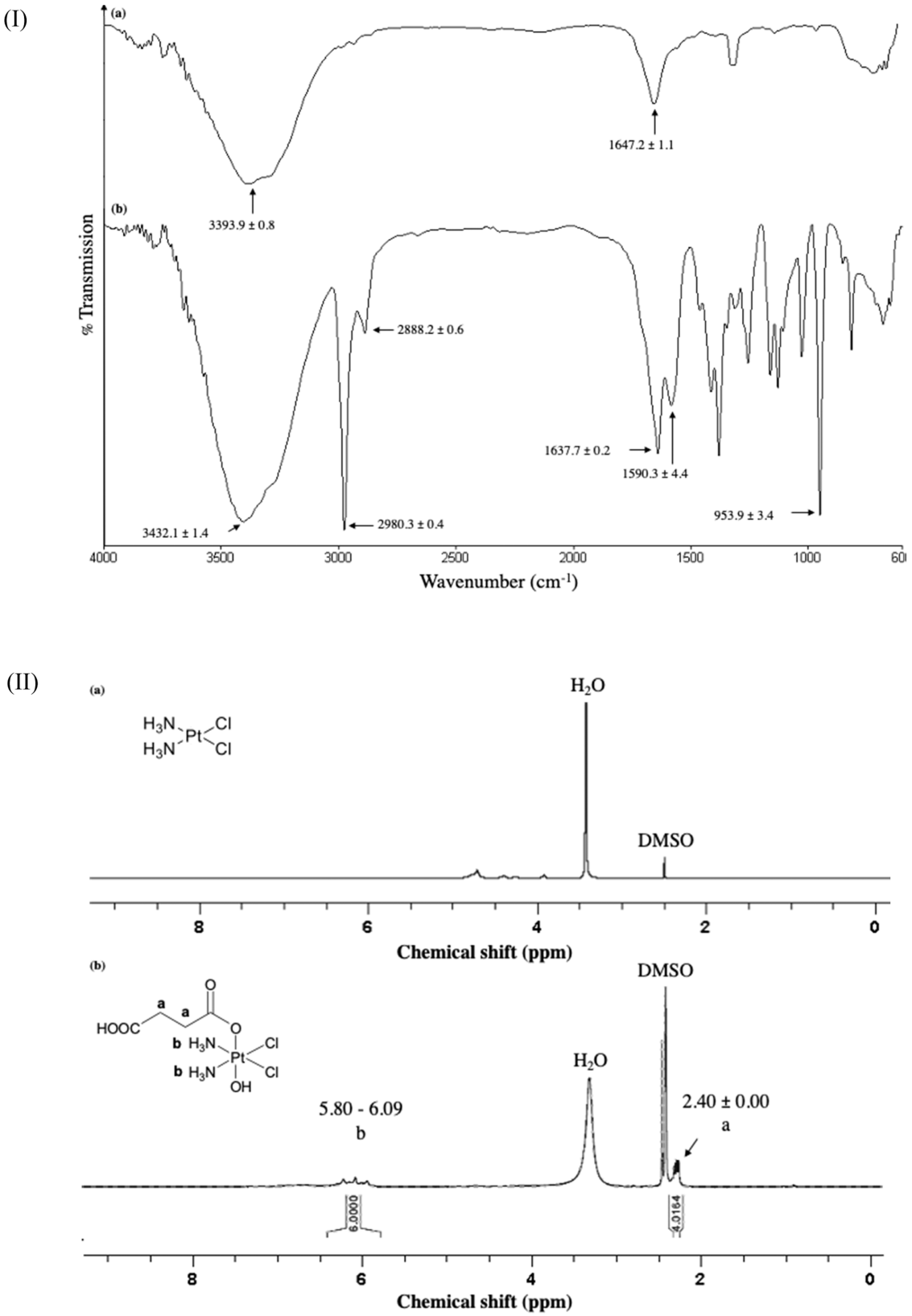

Figure 1. Profiles of (I) ATR-FTIR and (II) ^{1}HNMR spectra of (a) cisplatin and (b) CPT.

(Arg-Gly-Asp),[34,35] cyclic RPM (CPIEDRPMC)[34] and PCP (DPRATPGS)[29,34,35] (peptide), galactose[46] (simple sugar), and anisamide[47] (benzamide derivative) have been covalently grafted onto chitosan/amino-rich polymers and processed into nanomedicine. The nanomedicine adopts active and passive targeting approaches to deliver the drugs in vivo.[28,34,38,42,44,46,48−50] It raises drug accumulation at the tumor microenvironment with reduced systemic adverse effects at a lower required drug dose. An overview of literature from 2017 to 2022 indicated that most chitosans of conjugates were

https://doi.org/10.1021/acsomega.4c03529
ACS Omega 2025, 10, 2428−2441

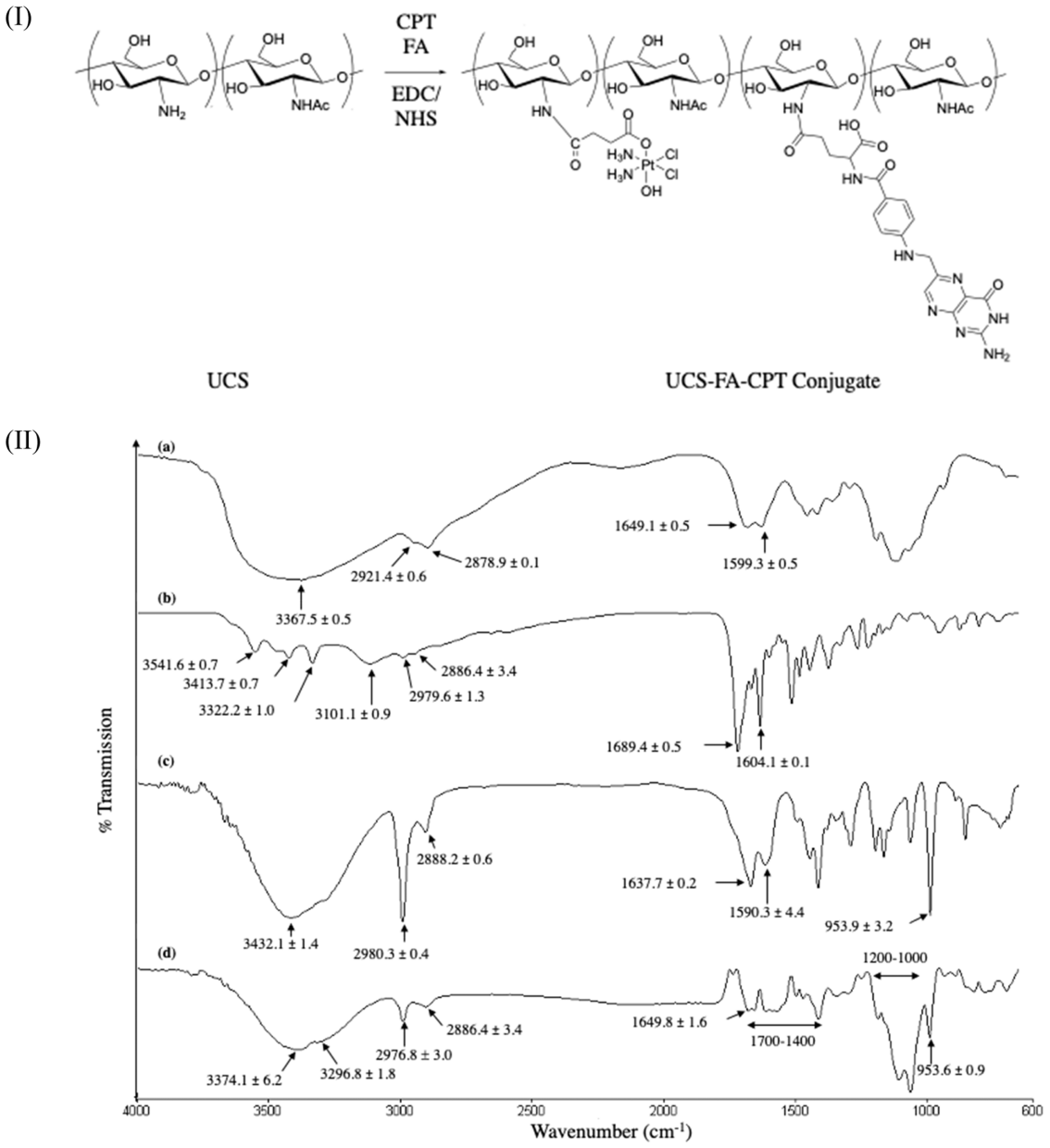

Figure 2. (I) Synthesis scheme of UCS-FA-CPT conjugate and (II) ATR-FTIR spectra of (a) UCS, (b) FA, (c) CPT, and (d) UCS-FA-CPT conjugate.

characterized by a molecular weight of 50−190 kDa and have a maximum of two ligands (drug and homing device) conjugating to their backbone.[28,38,39,41,44,47,48] The chitosan-drug-targeting ligand conjugate is foreseeably less soluble in the aqueous milieu, as most amino groups of chitosan participate in covalent conjugation and are not available to undergo protonation and form hydrogen bonding with the surrounding water molecules. Further, most drugs and targeting ligands such as 5-fluorouracil, paclitaxel, doxorubicin, methotrexate, camptothecin, docetaxel, folate, and estrone are relatively hydrophobic and bulky.[34,38,41,43,44] This in turn negates the solubilization process of chitosan conjugates.

Lower molecular weight chitosan is relatively soluble in the aqueous medium and has an inherent anticancer activity.[51] Thus, it is deemed favorable for use as a platform for cancer nanomedicine development. Preliminary trials in our laboratory indicated that conjugation of drug (i.e., cisplatin) and targeting ligand (i.e., folic acid) onto lower molecular weight chitosan however led to reduced aqueous solubility in deionized water, 0.1−2% v/v acetic acid solution, and phosphate-buffered saline, thus causing the processing of conjugate into nanomedicine requiring harmful and flammable organic solvents and altering its pharmacokinetics as well as pharmacodynamics performances in the tumor microenvironment. The solubility of chitosan has been improved through grafting with fatty acids, namely, linoleic acid or oleic acid onto chitosan of 250 kDa[52,53] and deoxycholic acid onto chitosan of 30 kDa.[51] The aqueous solubility of chitosan is enhanced via reducing the intermolecular hydrogen bonding of chitosan through the insertion of hydrophobic or bulky substituents without negating the chitosan−water hydrogen bonding.[54−56] The hydrophobic fragment can be separated from the aqueous exterior by entropic gain to form an inner core surrounded with a hydrophilic shell undergoing solvation by the aqueous

https://doi.org/10.1021/acsomega.4c03529
ACS Omega 2025, 10, 2428−2441

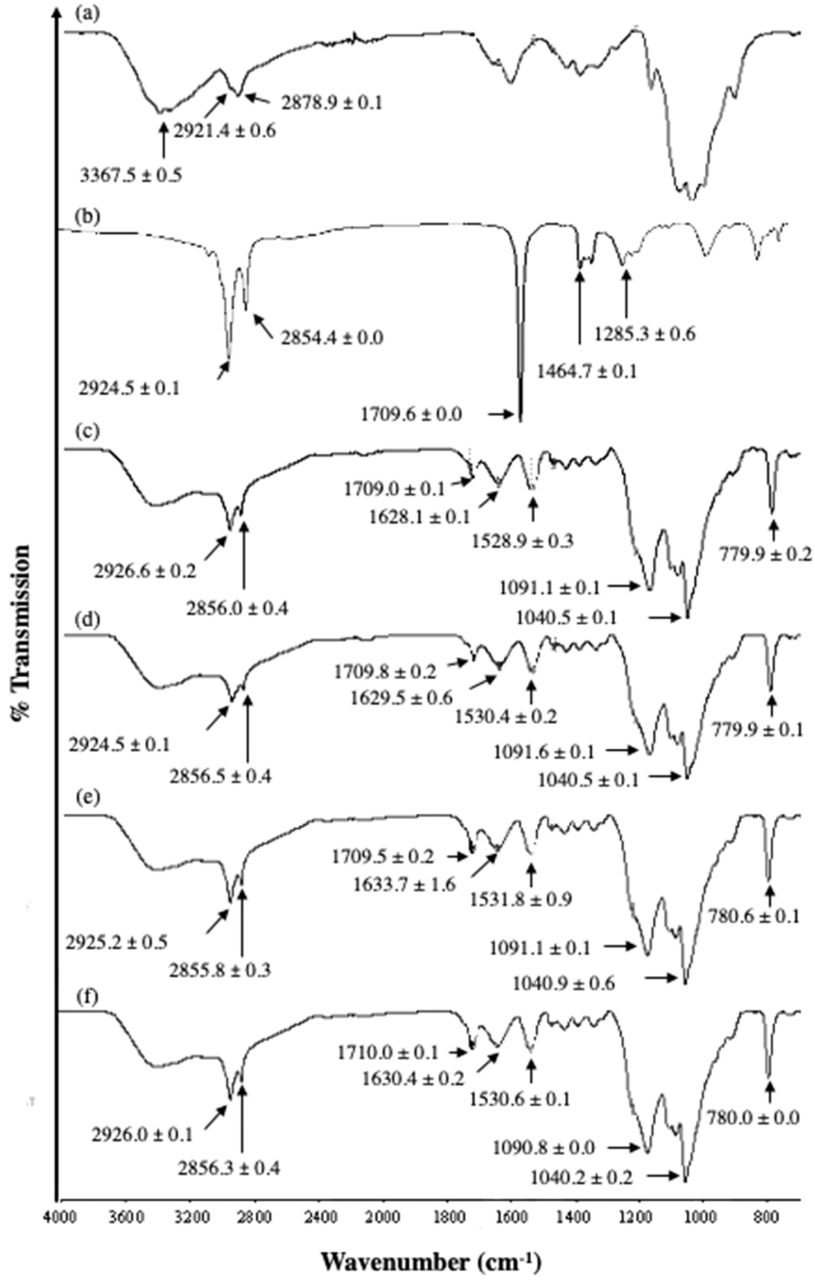

Figure 3. ATR-FTIR spectra of (a) UCS, (b) OA, (c) UCS-OA conjugate 1, (d) UCS-OA conjugate 2, (e) UCS-OA conjugate 3, and (f) UCS-OA conjugate 4.

medium.[55] With reference to drug and targeting ligand conjugate of lower molecular weight chitosan, specifically oligochitosan (<5 kDa), it is hypothesized that the spaces for covalent grafting the oligomeric backbone with fatty acid can be limited due to overcrowding of drug, targeting ligand, and fatty acid on the same oligochitosan backbone. The solubilizer function of fatty acid may not be expressed due to steric hindrance of drug and targeting ligand against the chitosan−fatty acid conjugate to orientate into a structure with a hydrophilic shell and hydrophobic core. On this note, this study aims to elucidate the challenges faced in the synthesis of oligochitosan conjugate using oleic acid, folic acid, and cisplatin as solubilizer, targeting ligand, and drug, respectively, and examine the solubility profiles of conjugate as a function of oleic acid.

RESULTS AND DISCUSSION

Preparation of Ultralow Molecular Weight Chitosan (UCS). Under the influence of microwave and electrolyte, the parent chitosan (weight-average molecular weight = 45,611 ± 145 Da, number-average molecular weight = 32,321 ± 726 Da, dispersity = 1.400 ± 0.026, degree of deacetylation = 88.4 ± 2.1% (FTIR); 93.5 ± 1.1% (NMR)) became shorter (weight-average molecular weight = 2685.66 ± 0.94 Da, number-average molecular weight = 2550.00 ± 6.38 Da, dispersity = 1.053 ± 0.002; Student's t test: $p < 0.05$) and was characterized by a degree of deacetylation of 96.3 ± 1.1% (FTIR) (98.0 ± 0.2% (NMR)) with a yield of 94.87 ± 2.10%. UCS was approximately 17 times shorter than the low molecular weight chitosan meeting the molecular weight classification of oligochitosan with a higher degree of

https://doi.org/10.1021/acsomega.4c03529
ACS Omega 2025, 10, 2428−2441

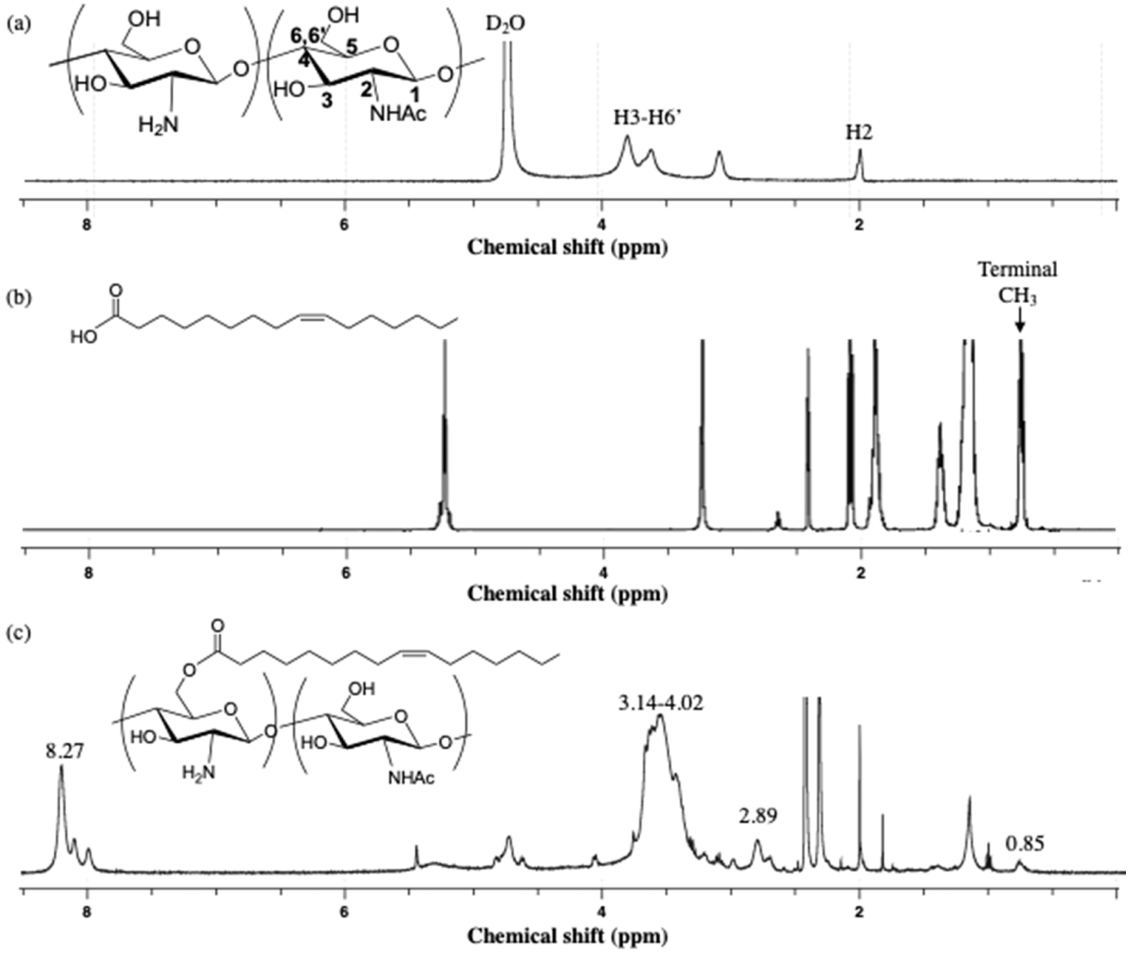

Figure 4. ^{1}H NMR spectra of (a) UCS, (b) OA, and (c) UCS-OA conjugate 1.

deacetylation. UCS was dissolvable in 0.1% v/v acetic acid solution (pH 3.3) and deionized water (pH 6.5). It is foreseeable to be processable in an aqueous milieu for nanoparticle development and able to be solubilized by the biological medium in the acidic tumor microenvironment (pH = 5.5−7[57]), which eases cellular transport.

Synthesis of UCS-Folate-Cisplatin (UCS-FA-CPT) Conjugate. UCS contains amino functional groups where folic acid can be covalently conjugated onto its parent chain via an amidation reaction involving the carboxylic acid groups of the latter. Cisplatin has two amino functional groups in each molecule. To enable cisplatin to conjugate with UCS, it was functionalized with a carboxylic acid moiety via the introduction of succinic anhydride. The cisplatin was characterized by FTIR peaks attributing to the N−H group at 3393.9 ± 0.8 and 1647.2 ± 1.1 cm^{-1} (Figure 1Ia). Successful succinylation of cisplatin was indicated by the development of FTIR peaks at 2980.3 ± 0.4 and 2888.2 ± 0.6 cm^{-1} due to the introduction of CH_2 moiety, and the formation of dual peaks at 1637.7 ± 0.2 and 1590.3 ± 4.4 cm^{-1} with transmission intensity being lower with peak at 1637.7 ± 0.2 cm^{-1} than that of 1590.3 ± 4.4 cm^{-1} due to the formation of carbonyl ester (Figure 1Ib). The wavenumber of the FTIR peak attributed to the N−H group at 3393.9 ± 0.8 cm^{-1} was increased to 3432.1 ± 1.4 cm^{-1}, following a reduction in inter−N−H interaction due to N−H interacting with the adjacent COOH group (Figure 1Ib). The succinylation evidence was further supported by ^{1}H NMR characteristics of cisplatin and its succinyl ester with chemical shift signals at δ 2.40 ± 0.00 ppm (m, 4H) and NH protons of CPT at δ 5.80−6.09 ppm (br, 6H) (Figure 1II). The signal at 3.33 ppm was assigned to the water residue present in DMSO-d_6.

Covalent grafting of CPT and FA onto UCS led to the formation of a conjugate with folate content and drug content of 5.34 ± 0.28 and 0.38 ± 0.55%, respectively (Figure 2I). The UCS-FA-CPT conjugate was dissolved poorly in 0.1% v/v aqueous acetic acid solution (pH 3.3), deionized water (pH 6.5), and phosphate-buffered saline pH 7.4. The same conjugate was not soluble in deuterated chloroform, methanol, benzene, acetonitrile, acetone, and dimethyl sulfoxide. Thus, it was not characterizable by the ^{1}H NMR spectroscopy technique. The conjugation of UCS-FA-CPT was reflected by FTIR analysis at the following peaks: 3374.1 ± 6.2 and 3296.8 ± 1.8 cm^{-1} attributing to O−H and N−H groups of UCS, CPT, and FA; 2976.8 ± 3.0 and 2886.4 ± 3.4 cm^{-1} attributing to C−H group of UCS and CPT; overlay peaks at 1400−1700 cm^{-1} ascribing to amide C═O group of UCS-CPT/UCS-FA (1649.8 ± 1.6 cm^{-1}); a broad peak between 1000 and 1200 cm^{-1} representing UCS and 953.6 ± 0.9 cm^{-1} ascribing CPT (Figure 2II).

Preparation of UCS-Oleate-Folate-Cisplatin (UCS-OA-FA-CPT) Conjugate. UCS-FA-CPT exhibited poor aqueous and organic solubilities, attributed to its polymeric nature and a high intramolecular binding affinity of UCS to the grafted CPT and FA via N−H and O−H moieties. The latter was reflected by the formation of an FTIR band with dual peak

https://doi.org/10.1021/acsomega.4c03529
ACS Omega 2025, 10, 2428−2441

characteristics at 3374.1 ± 6.2 and 3296.8 ± 1.8 cm^{-1} of which the wavenumbers were intermediate to those of UCS with FA and CPT or lower than the starting materials (Figure 2II). The introduction of OA onto the backbone of the UCS-FA-CPT conjugate was envisaged to introduce a relatively hydrophobic hydrocarbon-rich domain, thereby reducing its intramolecular bonding and converting the UCS-FA-CPT conjugate into an amphiphilic molecule dissolvable in an aqueous or organic milieu.

UCS-OA conjugate was first synthesized via selective *O*-acylation of UCS with oleoyl chloride in the presence of methanesulfonic acid to allow the amino groups of UCS to be available for covalent conjugation with FA and CPT in the subsequent reaction steps. Under *O*-acylation reaction condition, *N*-acylation of UCS was not mediated since the primary amino groups rapidly formed salt with the methanesulfonic acid molecules and were not available for acylation.

Oleic acid was characterized by FTIR peaks at 2924.5 ± 0.1 and 2854.4 ± 0.0 cm^{-1} denoting C−H group, 1709.6 ± 0.0 cm^{-1} denoting C═O group (COOH), and two broad bands between 1464.7 cm^{-1} ± 0.1 and 1285.3 ± 0.6 cm^{-1} ascribing to CH_3 and CH_2 deformation (Figure 3). The grafting of oleoyl group onto UCS was supported by FTIR spectra, which exhibited the OA characteristics at the corresponding average wavenumbers: 2925.6 ± 1.0 and 2856.2 ± 0.3 cm^{-1} denoting C−H moiety, 1709.6 ± 0.4 cm^{-1} denoting C═O moiety, and two broad bands between 1040.6 ± 0.3 and 1091.2 ± 0.3 cm^{-1} ascribing to CH_3 and CH_2 deformation. The grafting of oleic acid onto UCS was translated to the formation of FTIR dual peaks at 1630.4 ± 2.4 cm^{-1} attributing to the ester linkage developed through the oleoylation of UCS and 1530.4 ± 1.2 cm^{-1} attributing to the free amino group of UCS. A strong *O*-acyl peak was detected at 780.1 ± 0.3 cm^{-1}.[58] No *N*-acyl peak was detected at ∼2300 cm^{-1}.[59]

NMR analysis of UCS-OA conjugate indicated that OA was grafted onto UCS: 2.89 ppm ascribed to the H2 proton of chitosan; 3.14−4.02 ppm ascribed to the H3−H6 protons of chitosan; 0.85 ppm ascribed to the terminal methyl (CH_3) protons of oleic acid; 8.27 ppm ascribed to amino protons of chitosan (Figure 4[60]). The degree of oleoyl substitution increased with the molar ratio of oleoyl chloride to the glucosamine unit of UCS (Table 1). UCS-OA conjugate with a DS < 10% (weight-average molecular weight = 2979.50 ± 5.16 Da, number-average molecular weight = 2705.60 ± 10.99 Da, dispersity = 1.099 ± 0.001) was dissolvable in aqueous and organic media (Figure 5b). A rise in DS beyond 10% or more decreased the solvation tendency of the UCS-OA conjugate in the aqueous media (Figure 5c). These oleoyl-rich UCS, however, were soluble in dimethyl sulfoxide owing to their hydrophobic character that favored them being solvated by the organic medium (Figure 5c).

Table 1. Degree of the Oleoyl Substitution (DS) of UCS-OA Conjugates and Their Yields

UCS-OA conjugate	chitosan[a] (mmol)	oleoyl chloride (mmol)	DS (%)	yield (%)
1	1	0.05	7.37 ± 0.45	87.20 ± 3.45
2	1	0.20	12.38 ± 0.65	78.41 ± 5.05
3	1	0.8	30.63 ± 0.83	71.12 ± 4.92
4	1	1.2	47.00 ± 1.20	69.11 ± 3.82

[a]Based on the molecular weight of glucosamine unit of UCS at 161 g mol^{-1}.

To facilitate the design of a UCS-FA-CPT conjugate that is soluble in liquid medium for nanoparticle preparation and in acidic tumor microenvironment for efficient cellular interaction and uptake, UCS-OA-FA-CPT conjugate with a DS value of OA < 10% was developed. The folate content and drug content of the conjugate were 8.50 ± 0.57% and 0.94 ± 0.80%, respectively. The conjugate was characterized by weight-average molecular weight of 3882.66 ± 5.44 Da, number-average molecular weight of 3086.03 ± 23.95 Da, and dispersity of 1.258 ± 0.010. Grafting of UCS with OA, FA, and CPT increased its molecular size and translated to molecular species of varying sizes due to heterogeneity in chemical reactions. FTIR analysis indicated that a characteristic OA peak was evidently shown in the spectrum of the UCS-OA-FA-CPT conjugate at wavenumber between 1500 and 1700 cm^{-1} denoting the C═O moiety of OA (Figure 6). NMR analysis of UCS-OA-FA-CPT conjugate indicated that OA, FA, and CPT were grafted onto UCS: 2.40 ppm ascribed to the CH_2 of CPT, 0.86 ppm ascribed to the terminal methyl (CH_3) protons of OA, 1.07 and 1.24 ppm ascribed to CH_2 protons of OA, 6.57−8.63 ppm ascribed to aromatic protons of FA, and 3.64 ppm ascribed to the H3−H6′ protons of UCS (Figure 7). DS of OA in UCS-OA-FA-CPT conjugate was 4.51 ± 0.32%. Using the same molar ratio of oleoyl chloride to the glucosamine unit of UCS as UCS-OA conjugate that was initially substituted with 7.37 ± 0.45% of OA, a reduction in DS was due to subsequent UCS-OA bond hydrolysis during FA and CPT conjugation onto the UCS-OA chains. UCS, with a given short chain length, nonetheless was able to covalently conjugate with OA, FA, and CPT. The formed conjugate, unlike the OA-free counterpart, was dissolvable in 0.1% v/v acetic acid solution and dimethyl sulfoxide fully, and in distilled water and phosphate-buffered saline to great extents (Figure 5). The solubilization process of the UCS-OA-FA-CPT conjugate was deemed to be accompanied by reduced chain entanglement as suggested by reduced specific viscosity against that of UCS (Table A1). In comparison to the UCS-FA-CPT conjugate, the introduction of OA reduced the strength of hydrogen bonding of the conjugate. This was evidenced by an increase in the wavenumber of the UCS-OA-FA-CPT conjugate at 3380.9 ± 1.6 and 3299.7 ± 2.0 from 3374.1 ± 6.2 and 3296.8 ± 1.8 cm^{-1} in the case of the UCS-FA-CPT conjugate (Figure 6). OA is characterized by 1 hydrogen bond donor and 2 hydrogen bond acceptors unlike folic acid with 6 hydrogen bond donors and 10 hydrogen bond acceptors. It was hydrophobic and able to sterically hinder the interchain interaction with a lower tendency to develop chemical bonding, thus promoting the aqueous solubility of the UCS-FA-CPT conjugate.

Cytotoxicity Profiles. With the water-soluble feature, the UCS-OA-FA-CPT conjugate (degree of oleate substitution = 4.51 ± 0.32%; folate content = 8.50 ± 0.57%; cisplatin content = 0.94 ± 0.80%) can be easily solubilized in the acetic acid solution and spray-dried into spherical nanoparticles (size = 985.7 ± 10.5 nm; polydispersity index = 0.53 ± 0.23; ζ-potential = 45.20 ± 2.41; aspect ratio = 1.03 ± 0.03; surface roughness = 24.82 ± 1.29 Ra) (Figure 8). The ζ-potential of UCS-OA-FA-CPT conjugate nanoparticles was larger than that of UCS-OA-CPT conjugate nanoparticles (34.80 ± 0.66 mV) indicating that the particle surface is populated with a folate

https://doi.org/10.1021/acsomega.4c03529
ACS Omega 2025, 10, 2428−2441

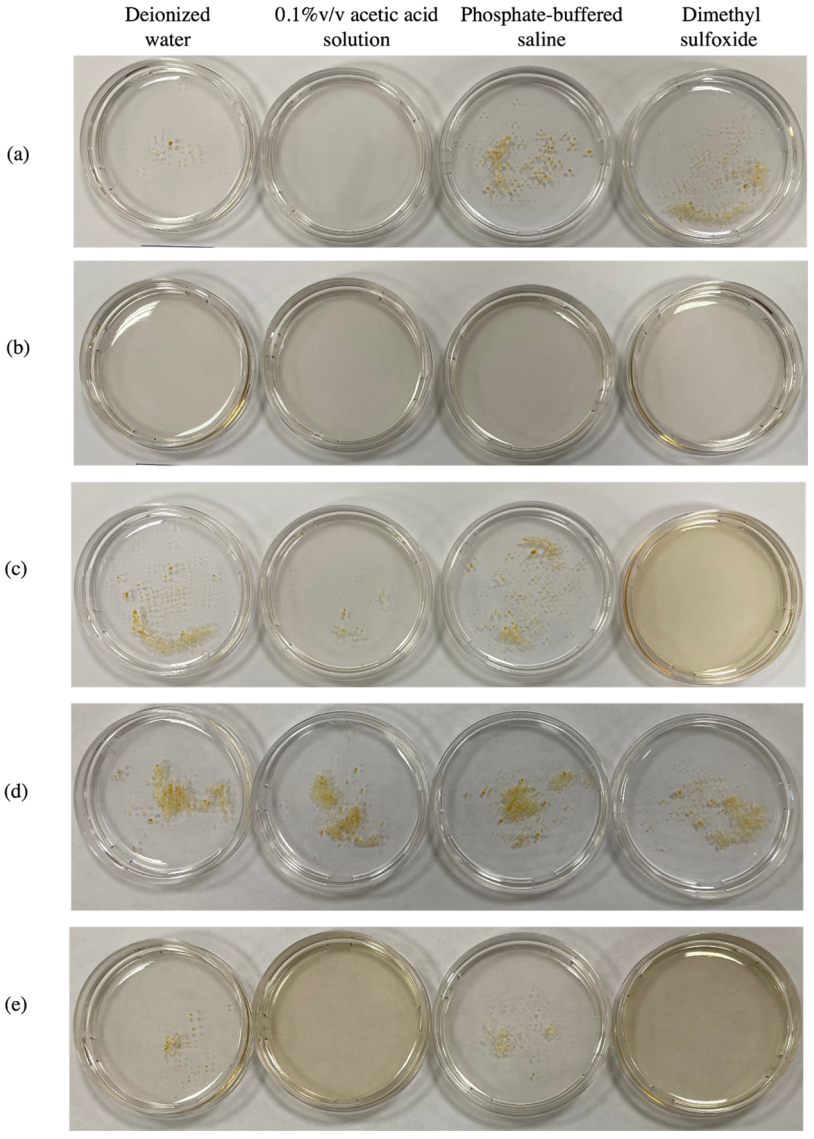

Figure 5. Solubility profiles of (a) UCS, (b) UCS-OA (7.37%) conjugate 1, (c) UCS-OA (47.00%) conjugate 4, (d) UCS-FA (5.34%)-CPT (0.38%) conjugate, and (e) UCS-OA (4.51%)-FA (8.50%)-CPT (0.94%) conjugate.

moiety. The viability of H1299 human lung cancer cells was reduced from 100.1 ± 2.3 to 50.5 ± 1.1% when they were treated with cisplatin (Figure 8). A further decrease in cancer cell viability to 10.3 ± 0.3% was obtained in cells receiving UCS-OA-FA-CPT conjugate nanoparticles at equivalent drug content. The ability to conjugate cisplatin onto the UCS-FA backbone and introduce OA to raise its water solubility enables one to prepare spray-dried nanoparticles that express a higher anticancer activity than the neat drug.

CONCLUSIONS

Combination effects of microwave irradiation and ionic strength converted low molecular weight chitosan into oligochitosan, an ultralow molecular weight variant. Grafting oligochitosan with folic acid and cisplatin translated to the formation of a conjugate that was poorly soluble in both aqueous and organic media. Grafting such a conjugate with oleic acid promoted its aqueous and organic solubilities through reducing the intramolecular binding affinity of oligochitosan to the grafted folate and cisplatin via N−H and O−H moieties. Co-conjugating oleic acid, folic acid, and cisplatin onto oligochitosan risks crowding and steric hindrance, which hinder the grafting process. On this note, oligochitosan-oleate conjugation was effected through *O*-acylation to provide amino groups of oligochitosan for folate and cisplatin grafting. A degree of oleic acid substitution (DS) lower than 10% was preferred as higher substitution degrees conferred hydrophobicity and reduced the aqueous solubility of the conjugate. Oligochitosan-oleate-folate-cisplatin conjugate with 4.51 ± 0.32% DS, 8.50 ± 0.57% folate content, and 0.94 ± 0.80% cisplatin content was dissolvable in dimethyl sulfoxide as well as aqueous media pH 3−7 which represent common processing pH in drug vehicle development and tumor microenvironmental pHs for drug action where conjugate solubilization is imperative for exertion of cytotoxic actions.

The present study highlighted the challenges in the synthesis of the oligochitosan-oleate-folate-cisplatin conjugate with reference to aqueous solubility that is expected to have a strong bearing on conjugate solubility for processing into nanoparticles and nanoparticle solubilization in the tumor microenvironment for exertion of cancer cytotoxic actions. It

https://doi.org/10.1021/acsomega.4c03529
ACS Omega 2025, 10, 2428−2441

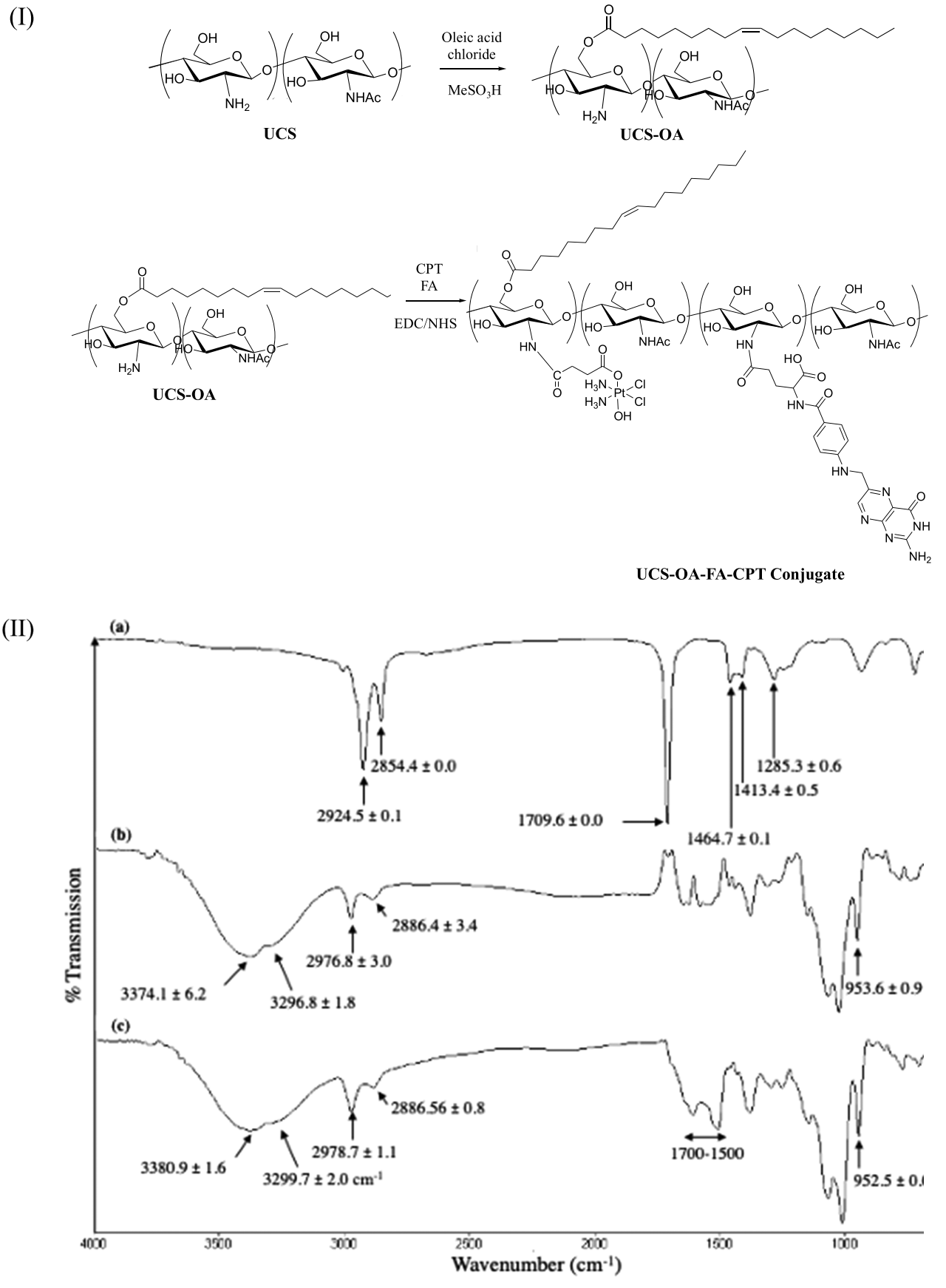

Figure 6. (I) Synthesis scheme of UCS-OA-FA-CPT conjugate and (II) ATR-FTIR spectra of (a) OA, (b) UCS-FA-CPT conjugate, and (c) UCS-OA-FA-CPT conjugate.

https://doi.org/10.1021/acsomega.4c03529
ACS Omega 2025, 10, 2428−2441

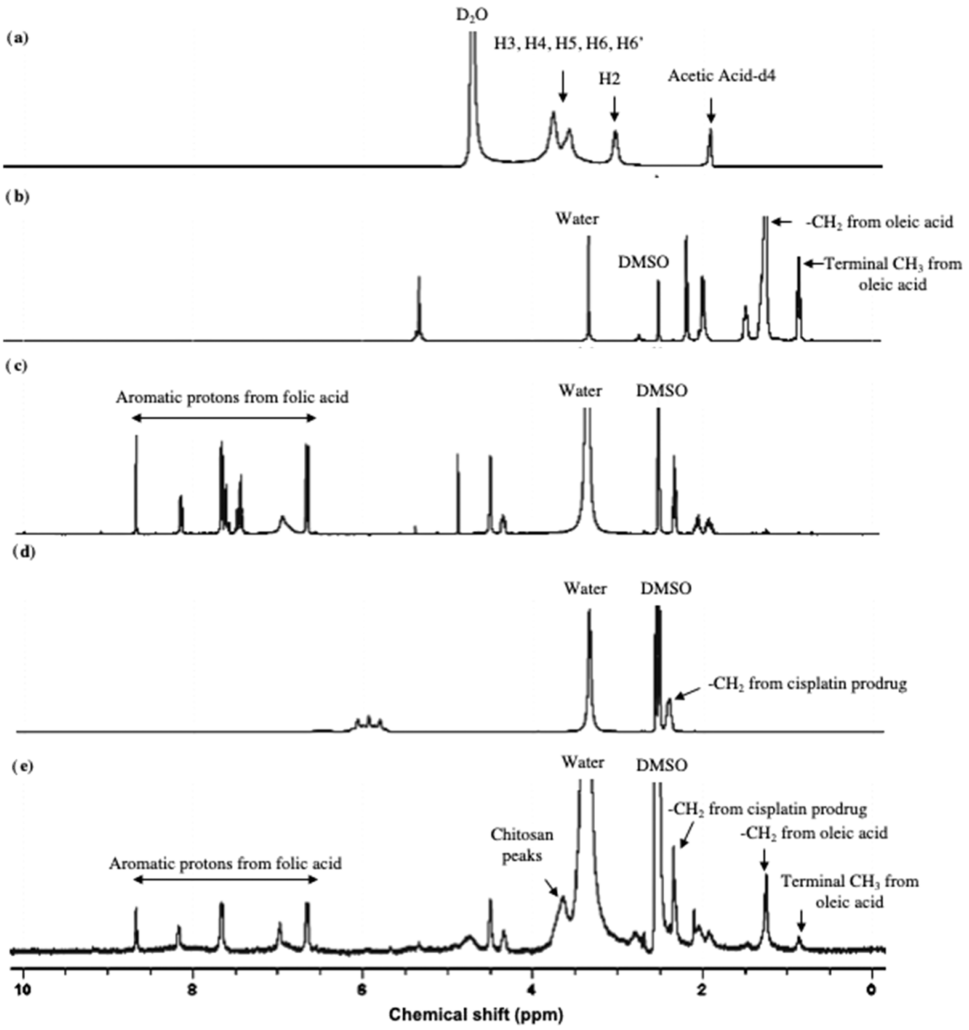

Figure 7. ^{1}H NMR spectra of (a) UCS, (b) OA, (c) FA, (d) CPT, and (e) UCS-OA-FA-CPT conjugate.

Table A1. Specific Viscosity of UCS and UCS-OA-FA-CPT Conjugate

	specific viscosity	
concentration (% w/w)	UCS	UCS-OA-FA-CPT conjugate
0.1	1.600 ± 0.000	0.103 ± 0.004
0.05	0.902 ± 0.004	0.067 ± 0.000
0.025	0.322 ± 0.004	0.042 ± 0.000
0.0125	0.183 ± 0.000	0.025 ± 0.000
0.0063	0.100 ± 0.007	0.008 ± 0.000

only provides a tentative biological implication. Relevant molecular biology and in vivo studies are required to elucidate the pharmacokinetics and pharmacodynamics properties of the oligochitosan-oleate-folate-cisplatin conjugate nanoparticles as a cancer therapeutic.

EXPERIMENTAL SECTION

Materials. Low molecular weight chitosan (CAS 9012−76−4; Zhejiang Aoxing Co. Ltd., China) was used as the polymeric backbone in conjugation with drug, targeting ligand, and solubilizer. Cisplatin (CAS 15663−27−1; Sigma-Aldrich, Germany) was selected as the drug of interest, with folic acid (CAS 59−30−3; FA, Sigma-Aldrich, Germany) as the targeting ligand and oleoyl chloride (CAS 112−77−6; Sigma-Aldrich, Germany) as the oleic acid derivative acting as the solubilizer to the conjugate. Acetic acid (CAS 64−19−7; Merck, Germany) was used to prepare the solvent for chitosan and its conjugates with tween 20 (CAS 9005−64−5; Fisher Scientific, U.K.) as the surfactant where applicable. Methanesulfonic acid (CAS 75−75−2; Sigma-Aldrich, Germany), acetone (CAS 67−64−1; Merck, Germany), *N*-hydroxysuccinimide (CAS 6066−82−6; NHS; Merck, Germany), 1-ethyl-3-(−3-(dimethylamino)propyl) carbodiimide hydrochloride (CAS 25952−53−8; EDC; Merck, Germany), anhydrous dimethyl sulfoxide (CAS 67−68−5; DMSO; Sigma-Aldrich, Germany), and hydrogen peroxide 30% (CAS 7722−84−1; Merck, Germany) were chemicals used in the conjugation reaction. Succinic anhydride (CAS 108−30−5) and dimethyl sulfoxide were used in the preparation of the cisplatin prodrug. Hydrochloric acid (CAS 7647−01−0), potassium chloride (CAS 7447−40−7) (Merck, Germany), and potassium bromide (CAS 7758−02−3; FTIR grade; Sigma-Aldrich, Germany) were used in molecular weight and degree of deacetylation analysis of chitosan. Deuterated dimethyl sulfoxide (CAS 2206−27−1, DMSO-d_6; Merck, Germany) was used as the solvent of conjugates in nuclear magnetic resonance spectroscopy analysis. Nitric acid 70% (CAS 7697−37−2; Trace metal grade; Fisher Scientific, UK) was used in the cisplatin content analysis.

https://doi.org/10.1021/acsomega.4c03529
ACS Omega 2025, 10, 2428−2441

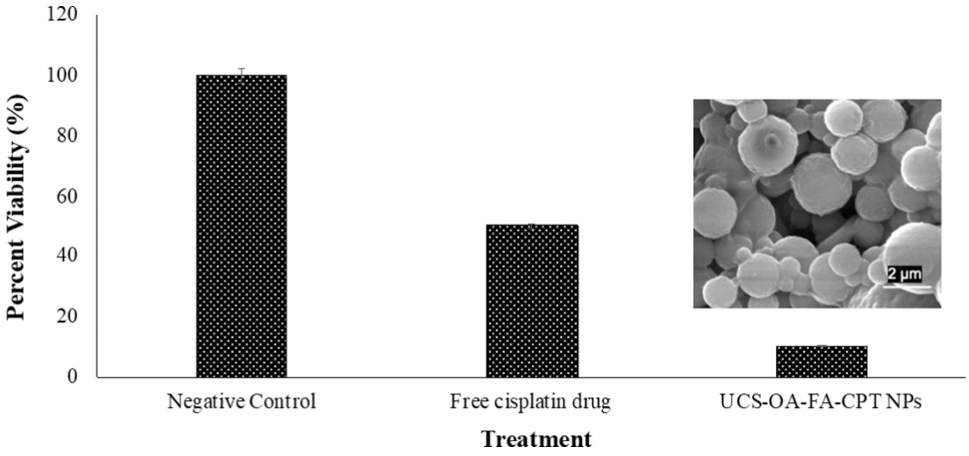

Figure 8. Scanning electron micrograph of UCS-OA-FA-CPT conjugate nanoparticles and their cytotoxicity profile against neat cisplatin in H1299 human lung cancer cells.

Synthesis and Characterization of Ultralow Molecular Weight Chitosan (UCS). *UCS Preparation.* UCS was prepared by subjecting the chitosan solution to microwave irradiation in a high ionic strength liquid as previously reported.[26] One gram of low molecular weight chitosan was dissolved in 49 g of 2% v/v acetic acid solution under continuous magnetic stirring at 25 ± 1 °C. The chitosan solution was added with 2 mL of 0.9% w/w sodium chloride solution and continued to stir for 1 h. The mixture was placed on a turntable of a microwave oven (EM-D953, Sanyo, Japan) at an off-center position. The solution was treated by microwave treatment at an irradiation power of 800 W for up to 9 min. It was covered with aluminum foil, cooled to ambient temperature, and had its pH adjusted to 7.5 using a 2 N sodium hydroxide solution. The chitosan in solution was precipitated using 96% ethanol (Fisher Scientific, U.K.). The chitosan precipitate was filtered (Whatman grade 1, Sigma-Aldrich), washed with distilled water, and subjected to hot air drying (Memmert, Germany) at 40 ± 1 °C for 24 h. The dried chitosan was conditioned in a silica gel desiccator at 25 ± 1 °C for at least 24 h prior to the determination of molecular weight and degree of deacetylation.

Molecular Weight Analysis. The apparent molecular weight of parent chitosan and UCS was determined using the gel permeation chromatography-refractive index detector technique (Agilent 1200 Series, Agilent Technologies Inc.) as previously reported by Nawaz and Wong.[61] A PL aquagel−OH mixed column (7.5 mm × 300 mm, 8 μm; Agilent Technologies, U.K.) was used with buffer pH 2.2 made of hydrochloric acid and potassium chloride as the mobile phase. The flow rate of the mobile phase and the column temperature were kept at 0.5 mL/min and 30 °C, respectively. Dextrans with molecular weights of 1000, 12,000, 50,000, 80,000, 150,000, 270,000, 410,000, 670,000, and 1,400,000 Da (Sigma-Aldrich, Denmark) were used as standards. A diluted chitosan solution at 2 mg/mL dissolved in 0.002% v/v acetic acid was prepared and filtered through a nylon syringe filter (pore diameter = 0.45 μm; GVS) before analysis. Number-average and weight-average molecular weights specific to gel permeation chromatography were determined with dispersity calculated as the quotient of the weight-average molecular weight to the number-average molecular weight. At least triplicates were carried out for each batch of sample, and the results were averaged.

Degree of Deacetylation Analysis. The degree of deacetylation (DD) of parent chitosan and UCS was determined using the Fourier transform infrared (FTIR) spectroscopy technique.[62−65] A mixture of chitosan and dry potassium bromide (weight ratio = 2:78) was ground into a fine powder using an agate mortar. The ground powder was compressed into a disc. Each disc was scanned at a resolution of 4 cm^{-1} over a wavenumber region of 450−4000 cm^{-1} using an FTIR spectrometer (Spectrum RX1 system, PerkinElmer). DD was calculated using the following equation:

$$DD = 100 - \left[\frac{A_{1655}}{A_{3450}} \times \frac{100}{1.33}\right] \quad (1)$$

where A = FTIR absorbance value at 1655 and 3450 cm^{-1} wavenumbers ascribing to amide-I of *N*-acetyl moiety and hydroxyl/amine moieties of the chitosan, respectively, and factor 1.33 = the value of A_{1655}/A_{3450} for a fully *N*-acetylated chitosan. At least triplicates were carried out for each batch of sample and the results were averaged.

The degree of deacetylation was also determined using the ^{1}H NMR method in accordance with the procedure reported by Hirai, Odani, and Nakajima.[66] Two milligrams of the sample was dissolved in 1 mL of 0.1% v/v deuterated acetic acid in deuterated water. The samples were transferred to NMR tubes and analyzed using a Fourier transform-NMR AVANCE III 400 MHz NMR spectrometer (Bruker, Germany) with tetramethylsilane as the internal standard. DD was calculated using the following equation:

$$DD = \left[1 - \left[\frac{1}{3}IHAc/\frac{1}{6}IH2{-}6\right]\right] \times 100 \quad (2)$$

where IHAc = integral intensity of acetyl group protons (HAc) and IH2−6 = integral intensity of protons H2, H3, H4, H5, H6, and H6′ (H2−6) of chitosan. HOD signal at 4.79 ppm was attributed to an exchange with the solvent deuteriums. At least triplicates were carried out for each batch of sample and the results were averaged.

Synthesis and Characterization of UCS Conjugates. *Synthesis of UCS-O-Oleate (UCS-OA) Conjugate.* UCS (161 mg) was dissolved in methanesulfonic acid solution (96%, 3 mL) at 25 ± 2 °C through continuous magnetic stirring for 20 min. Oleoyl chloride, at different equivalent weights of glucosamine unit of chitosan, was added into the UCS

https://doi.org/10.1021/acsomega.4c03529
ACS Omega 2025, 10, 2428−2441

solution (Table 1). The reaction mixture was stirred for 5 h. Thirty grams of crushed ice prepared from distilled water was subsequently added to the reaction mixture to terminate the reaction. The mixture was transferred into a centrifuge tube, diluted with acetone (20 mL), and subjected to centrifugation at 1000 rpm for 10 min (IEC Clinical Benchtop Centrifuge). The sediment was collected and washed twice with 14 mL of acetone followed by 14 mL of diethyl ether. It was dialyzed against dimethyl sulfoxide for 48 h at 25 °C to remove the excess oleoyl chloride and subsequently with deionized water for another 48 h to remove the methanesulfonic acid using the dialysis membrane (molecular weight cutoff: 1000 Da; Spectra/Por, Spectrum laboratories, Spain). The conjugate was then dried in a silica gel desiccator at 25 ± 2 °C.

Synthesis of Cisplatin Prodrug (CPT). The cisplatin prodrug, *cis,cis,trans*-[$Pt(NH_3)_2Cl_2(OH)$-$(O_2CCH_2CH_2CO_2H)$](CPT) was prepared using the method reported by Shi, Liu, Kerwood, Goodisman, and Dabrowiak.[67] A mixture of cisplatin (2 g, 6.67 mmol), hydrogen peroxide (30%, 11.37 mL, 100 mmol), and deionized water (90 mL) was heated to 60 °C under magnetic stirring at 1000 ± 32 rpm for 3 h in the dark. The mixture was cooled to room temperature and continued stirring for 16 h. The reaction mixture was concentrated under reduced pressure, and the product was allowed to precipitate at 4 °C over a week into a bright-yellow solid. The bright-yellow solid was collected by vacuum filtration, washed sequentially with ice-cold deionized water, ethanol, and diethyl ether, air-dried in the dark for 48 h, and further conditioned in a silica gel desiccator at 25 ± 1 °C until use.

In the second step, 0.2 g of bright-yellow solid (0.6 mmol) was dissolved in dimethyl sulfoxide (16 mL). The solution was added to succinic anhydride (0.06 g, 0.6 mmol). The reaction mixture was subjected to continuous magnetic stirring at 1000 ± 32 rpm and 25 ± 1 °C for 18 h. It was lyophilized using a freeze-dryer (α 1−2 LDplus, Martin Christ, Germany) at −40 °C under 0.1 mbar for 24 h. The light-yellow solid CPT was washed three times with 10 mL of acetone and 10 mL of diethyl ether followed by air drying and further conditioned in a silica gel desiccator at 25 ± 1 °C until use.

Synthesis of UCS-Oleate-Folate-Cisplatin (UCS-OA-FA-CPT) and UCS-FA-CPT Conjugates. Briefly, 161 mg of UCS or UCS-OA conjugate (degree of OA substitution, DD = 7.37 ± 0.45%) was dissolved in 10 mL of anhydrous dimethyl sulfoxide. FA (0.177 g, 0.4 mmol), NHS (0.046 g, 0.4 mmol), and EDC (0.040 g, 0.4 mmol) were dissolved in 3 mL of anhydrous dimethyl sulfoxide. Cisplatin prodrug (CPT) (0.174 g, 0.4 mmol), NHS (0.046 g, 0.4 mmol), and EDC (0.04 g, 0.40 mmol) were separately dissolved in 3 mL of anhydrous dimethyl sulfoxide. The folic acid and cisplatin prodrug mixtures were individually added dropwise into the UCS or UCS-OA conjugate solution and subjected to further magnetic stirring for 48 h in the dark at 25 ± 1 °C. The resultant mixture was coagulated by 300 mL of acetone and centrifuged (PK121 R, ALC) at 3400 rpm for 5 min. The supernatant was discarded, and the solid sediment was collected. The solid sediment was purified by dialysis against dimethyl sulfoxide for 48 h and subsequently with deionized water for another 48 h at 25 °C to remove the excess EDC, NHS, FA, and CPT using a dialysis membrane (molecular weight cutoff: 1000 Da; Spectra/Por, Spectrum laboratories, Spain). It was freeze-dried (−40 °C, 0.1 mbar; α 1−2 LDplus, Martin Christ, Germany) and further conditioned in a silica gel desiccator at 25 ± 1 °C until use. The yields of UCS-FA-CPT and UCS-OA-FA-CPT were 58.20 ± 7.14 and 48.50 ± 4.05%, respectively.

Nuclear Magnetic Resonance (NMR) Spectroscopy Analysis. Two milligrams of conjugate, prodrug, or starting material was dissolved in 1 mL of deuterated dimethyl sulfoxide and transferred into a 5 mm NMR tube. The sample was analyzed using a Fourier transform-NMR AVANCE III 400 MHz NMR spectrometer (Bruker, Germany) with tetramethylsilane as the internal standard. At least triplicates were carried out, and the results were averaged.

Fourier Transform Infrared (FTIR) Spectroscopy Analysis. One milligram of conjugate, prodrug, or starting material was scanned over a wavenumber range of 450−4000 cm^{-1} with FTIR spectrometer (Spectrum RX1 FTIR system, PerkinElmer) using MIRacle ATR accessory (PIKE Technologies, Madison). The characteristic peaks of infrared transmission spectra of the samples were recorded at a resolution of 16 cm^{-1} over a wavenumber region of 450−4000 cm^{-1} with an acquisition time of 1.5 min. At least triplicates were carried out and the results were averaged.

Molecular Weight Analysis. The molecular weight profiles of soluble UCS-OA and UCS-OA-FA-CPT conjugates were determined using the test protocol outlined in the section on UCS synthesis.

Degree of Substitution of Oleic Acid Analysis. The degree of substitution (DS) of oleic acid was determined from the ^1H NMR spectra of UCS-OA conjugates.[58] It was calculated using eq 3 as follows:

$$\mathrm{DS} = \frac{\text{integral at } \delta\ 0.85}{3 \times \text{integral at } \delta\ 2.89} \times 100\% \tag{3}$$

where δ 0.85 and δ 2.89 are the ^1H NMR peak area of CH_3 of oleoyl and H_2 of chitosan, respectively. At least triplicates were carried out and the results were averaged.

FA Content Analysis. Two milligrams of UCS-OA-FA-CPT conjugate or UCS-FA-CPT conjugate was dissolved in 0.01 M hydrochloric acid solution overnight in the dark at 25 ± 1 °C. The pH of the dissolved conjugate was adjusted to 10 using 0.1 M sodium hydroxide solution. The folate content of conjugates was analyzed at the wavelength maxima of 365 nm using a UV−visible spectrophotometer (extinction coefficient: 27614; Cary 50 Conc. Varian Australia Pty. Ltd., Australia) with UCS-OA-CPT and UCS-CPT as controls. The results were taken as an average of three readings.

CPT Content Analysis. One milligram of UCS-OA-FA-CPT conjugate or UCS-FA-CPT conjugate was digested in 1 mL of 70% nitric acid at 95 °C for 2 h. The digested conjugates were diluted 100-fold with the final platinum concentration within the working range of 0.1−100 $\mu g\ L^{-1}$ with Milli-Q water. The platinum content was determined by an inductively coupled plasma mass spectrometer (ICPMS 7500 Single Turbo System, Agilent). The most abundant isotope of platinum was monitored at m/z = 195. The experiment was conducted in triplicate, and the results were taken as an average of three readings.

Solvation Analysis. Fifty milligrams of UCS, UCS-OA conjugate, UCS-FA-CPT conjugate, or UCS-OA-FA-CPT conjugate was suspended in 5 mL of deionized water, 0.1% v/v acetic acid solution, phosphate-buffered saline pH 7.0 (Fisher Scientific, U.K.), and dimethyl sulfoxide of which represented the common solvents employed in nanoprocessing

https://doi.org/10.1021/acsomega.4c03529
ACS Omega 2025, 10, 2428−2441

and analysis. They were subjected to sonication at 25 ± 1 °C for 3 × 10 min with a 2 min rest interval between each sonication in a tightly sealed vial. The solvation status of UCS and its conjugates was recorded following 24 h of standing at 25 ± 1 °C. A soluble sample was defined by complete solubilization with no detectable solid residue. A poorly soluble sample was defined by the presence of solid particles. Its insolubility profile was verified through further incubation at 40 °C for 3 h.

Solution Viscosity Analysis. The UCS and UCS-OA-FA-CPT conjugates were dissolved in 0.1% v/v acetic acid solution to form 0.1, 0.05, 0.025, 0.0125, and 0.0063% w/w polymer solutions. The viscosity of the solutions was examined using a U-tube (size B, Poulten Self-e & Lee Ltd., U.K.) at 30.0 ± 0.5 °C. The specific viscosity of the UCS and UCS-OA-FA-CPT conjugate solutions was calculated using the following equation:

$$\text{specific viscosity} = \frac{F - F_0}{F_0} \quad (4)$$

where F is the flow time of the test solution and F_0 is the flow time of 0.1% v/v acetic acid solution that was used as the solvent for the test sample. Triplicates were conducted, and the results were averaged.

Cytotoxicity Study. *Preparation of UCS-OA-FA-CPT Nanoparticles.* An accurately weighed 100 mg (0.1% w/w) of UCS-OA-FA-CPT conjugate and 10 mg (0.01% w/w) of tween 20 were dissolved in 99.89 g of 1% v/v acetic acid solution under magnetic stirring at 2083 ± 32 rpm for 2 h. The resultant solution was then nanospray-dried using a nanospray dryer (TwinNanoSpray, UiTM, Malaysia) adapting the following operating parameters: inlet temperature = 70 °C, outlet temperature = 24 °C, solution feed rate = 2.92 g/min, concurrent airflow = 2−2.5 m/s, and atomizing air pressure = 6 bar. The spray-dried powder was harvested from the collecting electrode using a rubber spatula. The sample was kept in a sealed vial and placed in a desiccator at 25 °C until use.

Size and ζ-Potential Analysis. One milligram of UCS-OA-FA-CPT conjugate nanoparticles was dispersed in 15 mL of 95% ethanolic solution through brief sonication. The size and ζ-potential were measured by photon correlation spectroscopy (Nano ZS 90, Malvern Instruments Ltd., U.K.) at 25 °C in a quartz cell and ζ-potential cell, respectively. Scattered light was detected at a scattering angle of 90°. Triplicates were conducted, and the results were averaged.

Morphology Analysis. The shape and surface morphology of UCS-OA-FA-CPT conjugate nanoparticles were examined using a scanning electron microscope (Quanta 450 FEG, FEI, The Netherlands). The sample was first adhered to carbon tape. It was then platinum sputter-coated (JEOL JFC-1600, Jeol, Japan) and subjected to microscopic examination at an accelerating voltage of 5 kV. The particle shape was defined by the aspect ratio deriving from the quotient of length to breadth of a particle. The surface roughness of nanoparticles was analyzed using ImageJ-win32 software, employing the "Analysis Particle" and "Roughness Calculation" modes. The arithmetic mean roughness (Ra) of the nanoparticles was calculated from nine measurements across three images, and the results were averaged.

MTT Assay. The folate receptor-expressed NCI-H1299 human nonsmall cell lung cancer cell line (ATCC) was cultured in 25 cm^2 cell culture flask (Nunclon, Thermo Fisher Scientific, Denmark) containing RPMI 1640 medium (supplemented with 10% fetal bovine serum, 100 unit/mL penicillin, and 100 μg/mL streptomycin) and incubated (CO_2CELL 170, MMM, Germany) at 37 °C with 5% carbon dioxide under humidified conditions. The cell culture medium was replaced every 48 h. At 80% confluency, the cells were washed twice with prewarmed phosphate buffer saline pH 7.4. One mL of trypsin-EDTA (CAS 9002−07−7; Sigma-Aldrich, Denmark) was added to the cells and further incubated for 5 min at 37 °C. The cells were suspended in 2 mL of cell culture medium. The cell suspension was centrifuged at 1500 rpm for 5 min (Multispeed centrifuge PK 121R, ALC International, Italy). The pellet was harvested and resuspended in an appropriate volume of the cell culture medium.

The cytotoxicity of UCS-OA-FA-CPT conjugate nanoparticles was evaluated in vitro using an MTT assay against the drug-treated group and the control group receiving no treatment. The resuspended H1299 cells were introduced into a sterile 96-well plate (Nunc, Denmark) at a density of 1×10^5 cells/well and incubated in a complete RPMI 1640 medium for 24 h at 5% carbon dioxide ambiance and 37 °C to promote cell adhesion. The medium was then replaced by 100 μL of UCS-OA-FA-CPT conjugate nanoparticles or cisplatin at a final equivalent platinum concentration of 11.25 μg/mL in a complete RPMI 1640 medium. The incubation was continued for 48 h. Then, 20 μL of MTT reagent solution (CAS 298−93−1; 0.5 mg/mL in phosphate buffer saline pH 7.4) was added with further 4 h incubation in darkness. The culture medium was subsequently removed. A volume of 100 μL of DMSO was added to each well and shaken for 15 min to dissolve the formed formazan crystals. The absorbance of the formazan product was determined at 570 nm by a microplate reader (POLARstar Omega, BMG Labtech, Germany). The cell viability was defined as the absorbance ratio of the treated sample (n = 6) to that of the control, expressed in percentage.

AUTHOR INFORMATION

Corresponding Authors

Chin Fei Chee − *Nanotechnology and Catalysis Research Centre, Universiti Malaya, 50603 Kuala Lumpur, Malaysia*; Email: cheechinfei@um.edu.my

Noorsaadah Abdul Rahman − *Department of Chemistry, Faculty of Science, Universiti Malaya, 50603 Kuala Lumpur, Malaysia; Institute for Advanced Studies, Universiti Malaya, 50603 Kuala Lumpur, Malaysia*; Email: noorsaadah@um.edu.my

Tin Wui Wong − *Non-Destructive Biomedical and Pharmaceutical Research Centre, Smart Manufacturing Research Institute, Universiti Teknologi MARA Selangor, 42300 Puncak Alam, Selangor, Malaysia; Particle Design Research Group, Faculty of Pharmacy, Universiti Teknologi MARA Selangor, 42300 Puncak Alam, Selangor, Malaysia; Department of Industrial Pharmacy, Faculty of Pharmacy, Silpakorn University, Nakhon Pathom 73000, Thailand;* orcid.org/0000-0002-9131-6937; Email: wongtinwui@uitm.edu.my

Author

M. Tamilarasi Muniandy − *Department of Chemistry, Faculty of Science, Universiti Malaya, 50603 Kuala Lumpur, Malaysia; Non-Destructive Biomedical and Pharmaceutical Research Centre, Smart Manufacturing Research Institute,*

https://doi.org/10.1021/acsomega.4c03529
ACS Omega 2025, 10, 2428−2441

Universiti Teknologi MARA Selangor, 42300 Puncak Alam, Selangor, Malaysia

Complete contact information is available at: https://pubs.acs.org/10.1021/acsomega.4c03529

Author Contributions

Conceptualization: T.W.W.; methodology: T.W.W., C.F.C., M.T.M.; validation: M.T.M., T.W.W., C.F.C., N.A.R.; formal analysis: M.T.M., T.W.W., C.F.C., N.A.R.; resources: N.A.R., T.W.W.; data curation: M.T.M.; writing original draft: M.T.M.; writing review and editing: T.W.W., C.F.C., N.A.R.; supervision: C.F.C., T.W.W., N.A.R.

Notes

The authors declare no competing financial interest.

■ ACKNOWLEDGMENTS

The authors wish to express their heartfelt thanks to Universiti Malaya (RU001B-2021), Universiti Teknologi MARA (0141903; IF0402Q1226), and the Ministry of Higher Education Malaysia (LRGS-NanoMITe RU029-2014) for funding and facility support.

■ REFERENCES

(1) Oladzadabbasabadi, N.; Nafchi, A. M.; Ariffin, F.; Wijekoon, J. O.; Al-Hassan, A. A.; Dheyab, M. A.; Ghasemlou, M. Recent advances in extraction, modification, and application of chitosan in packaging industry. *Carbohydr. Polym.* **2022**, *277*, No. 118876.

(2) Alhodieb, F. S.; Barkat, M. A.; Barkat, H. A.; Ab Hadi, H.; Khan, M. I.; Ashfaq, F.; Rahman, M. A.; Hassan, M. Z.; Alanezi, A. A. Chitosan-modified nanocarriers as carriers for anticancer drug delivery: Promises and hurdles. *Int. J. Biol. Macromol.* **2022**, *217*, 457−469, DOI: 10.1016/j.ijbiomac.2022.06.201.

(3) Andreica, B. I.; Cheng, X.; Marin, L. Quaternary ammonium salts of chitosan. A critical overview on the synthesis and properties generated by quaternization. *Eur. Polym. J.* **2020**, *139*, No. 110016.

(4) Fabiano, A.; Beconcini, D.; Migone, C.; Piras, A. M.; Zambito, Y. Quaternary ammonium chitosans: The importance of the positive fixed charge of the drug delivery systems. *Int. J. Mol. Sci.* **2020**, *21* (18), No. 6617.

(5) Freitas, E. D.; Moura, C. F., Jr; Kerwald, J.; Beppu, M. M. An overview of current knowledge on the properties, synthesis and applications of quaternary chitosan derivatives. *Polymers* **2020**, *12* (12), No. 2878.

(6) Jain, S. K.; Shilpi, S. Chitosan for advancing drug delivery. *Drug Delivery* **2017**, 293−340.

(7) Li, X.; Xing, R.; Xu, C.; Liu, S.; Qin, Y.; Li, K.; Yu, H.; Li, P. Immunostimulatory effect of chitosan and quaternary chitosan: A review of potential vaccine adjuvants. *Carbohydr. Polym.* **2021**, *264*, No. 118050.

(8) Lunkov, A.; Shagdarova, B.; Lyalina, T.; Dubinnyi, M. A.; Karpova, N.; Lopatin, S.; Il'ina, A.; Varlamov, V. Simple method for ultrasound assisted ≪click≫ modification of azido-chitosan derivatives by CuAAC. *Carbohydr. Polym.*, **2022**, *282*, No. 119109.

(9) Layek, B.; Mandal, S. Natural polysaccharides for controlled delivery of oral therapeutics: a recent update. *Carbohydr. Polym.* **2020**, *230*, No. 115617.

(10) Gonçalves, C.; Ferreira, N.; Lourenço, L. Production of low molecular weight chitosan and chitooligosaccharides (COS): A review. *Polymers* **2021**, *13* (15), No. 2466.

(11) Melro, E.; Antunes, F. E.; da Silva, G. J.; Cruz, I.; Ramos, P. E.; Carvalho, F.; Alves, L. Chitosan films in food applications. tuning film properties by changing acidic dissolution conditions. *Polymers* **2021**, *13* (1), No. 1.

(12) Qiao, C.; Ma, X.; Wang, X.; Liu, L. Structure and properties of chitosan films: Effect of the type of solvent acid. *LWT* **2021**, *135*, No. 109984.

(13) Panda, P. K.; Dash, P.; Chang, Y. H.; Yang, J. M. Improvement of chitosan water solubility by fumaric acid modification. *Mater. Lett.* **2022**, *316*, No. 132046.

(14) Kou, S. G.; Peters, L.; Mucalo, M. Chitosan: A review of molecular structure, bioactivities and interactions with the human body and micro-organisms. *Carbohydr. Polym.* **2022**, *282*, No. 119132.

(15) Nawaz, A.; Wong, T. W.Chitosan as Anticancer Compound and Nanoparticulate Matrix for Cancer Therapeutics. In *Encyclopedia of Marine Biotechnology*; Wiley, 2020; Vol. 3, pp 1737−1752.

(16) Pestov, A.; Bratskaya, S. Chitosan and its derivatives as highly efficient polymer ligands. *Molecules* **2016**, *21* (3), No. 330.

(17) Zhai, X.; Li, C.; Ren, D.; Wang, J.; Ma, C.; El-Aty, A. M. A. The impact of chitooligosaccharides and their derivatives on the in vitro and in vivo antitumor activity: A comprehensive review. *Carbohydr. Polym.* **2021**, *266*, No. 118132.

(18) Naveed, M.; Phil, L.; Sohail, M.; Hasnat, M.; Baig, M. M. F. A.; Ihsan, A. U.; Shumzaid, M.; Kakar, M. U.; Khan, T. M.; Akabar, M. D.; Hussain, M. I.; Zhou, Q.-G. Chitosan oligosaccharide (COS): An overview. *Int. J. Biol. Macromol.* **2019**, *129*, 827−843.

(19) Azuma, K.; Osaki, T.; Minami, S.; Okamoto, Y. Anticancer and anti-inflammatory properties of chitin and chitosan oligosaccharides. *J. Funct. Biomater.* **2015**, *6* (1), 33−49.

(20) Journot, C. M. A.; Nicolle, L.; Lavanchy, Y.; Gerber-Lemaire, S. Selection of water-soluble chitosan by microwave-assisted degradation and pH-controlled precipitation. *Polymers* **2020**, *12* (6), No. 1274.

(21) Ways, T. M.; Lau, W. M.; Khutoryanskiy, V. V. Chitosan and its derivatives for application in mucoadhesive drug delivery systems. *Polymer* **2018**, *10* (3), No. 267.

(22) Lim, C.; Hwang, D. S.; Lee, D. W. Intermolecular interactions of chitosan: Degree of acetylation and molecular weight. *Carbohydr. Polym.* **2021**, *259*, No. 117782.

(23) Entezar-Almahdi, E.; Mohammadi-Samani, S.; Tayebi, L.; Farjadian, F. Recent advances in designing 5-fluorouracil delivery systems: a stepping stone in the safe treatment of colorectal cancer. *Int. J. Nanomed.* **2020**, *15*, 5445−5458.

(24) Horo, H.; Das, S.; Mandal, B.; Kundu, L. M. Development of a photoresponsive chitosan conjugated prodrug nano-carrier for controlled delivery of antitumor drug 5-fluorouracil. *Int. J. Biol. Macromol.* **2019**, *121*, 1070−1076.

(25) Musalli, A. H.; Talukdar, P. D.; Roy, P.; Kumar, P.; Wong, T. W. Folate-induced nanostructural changes of oligochitosan nanoparticles and their fate of cellular internalization by melanoma. *Carbohydr. Polym.* **2020**, *244*, No. 116488.

(26) Nawaz, A.; Wong, T. W. Chitosan-carboxymethyl-5-fluorouracil-folate conjugate particles: microwave modulated uptake by skin and melanoma cells. *J. Invest. Dermatol.* **2018**, *138* (11), 2412−2422.

(27) Ak, G. Covalently coupling doxorubicin to polymeric nanoparticles as potential inhaler therapy: In vitro studies. *Pharm. Dev. Technol.* **2021**, *26* (8), 890−898.

(28) Escareño, N.; Hassan, N.; Kogan, M. J.; Juárez, J.; Topete, A.; Daneri-Navarro, A. Microfluidics-assisted conjugation of chitosan-coated polymeric nanoparticles with antibodies: Significance in drug release, uptake, and cytotoxicity in breast cancer cells. *J. Colloid Interface Sci.* **2021**, *591*, 440−450.

(29) Saeed, R. M.; Dmour, I.; Taha, M. O. Stable chitosan-based nanoparticles using polyphosphoric acid or hexametaphosphate for tandem ionotropic/covalent crosslinking and subsequent investigation as novel vehicles for drug delivery. *Front. Bioeng. Biotechnol.* **2020**, *8*, No. 4.

(30) Moradnia, H.; Raissi, H.; Shahabi, M. The performance of the single-walled carbon nanotube covalently modified with polyethylene glycol to delivery of Gemcitabine anticancer drug in the aqueous environment. *J. Biomol. Struct. Dyn.* **2021**, *39* (3), 881−888.

(31) Fathi, M.; Barar, J.; Erfan-Niya, H.; Omidi, Y. Methotrexate-conjugated chitosan-grafted pH-and thermo-responsive magnetic nanoparticles for targeted therapy of ovarian cancer. *Int. J. Biol. Macromol.* **2020**, *154*, 1175−1184.

(32) Shakeran, Z.; Keyhanfar, M.; Varshosaz, J.; Sutherland, D. S. Biodegradable nanocarriers based on chitosan-modified mesoporous

silica nanoparticles for delivery of methotrexate for application in breast cancer treatment. *Mater. Sci. Eng.: C* **2021**, *118*, No. 111526.
(33) He, R.; Yin, C. Trimethyl chitosan based conjugates for oral and intravenous delivery of paclitaxel. *Acta Biomater.* **2017**, *53*, 355−366.
(34) Jaiswal, S.; Dutta, P. K.; Kumar, S.; Chawla, R. Chitosan modified by organo-functionalities as an efficient nanoplatform for anti-cancer drug delivery process. *J. Drug Delivery Sci. Technol.* **2021**, *62*, No. 102407.
(35) Alizadeh, L.; Zarebkohan, A.; Salehi, R.; Ajjoolabady, A.; Rahmati-Yamchi, M. Chitosan-based nanotherapeutics for ovarian cancer treatment. *J. Drug Targeting* **2019**, *27* (8), 839−852.
(36) Cao, J.; Zheng, H.; Hu, R.; Liao, J.; Fei, Z.; Wei, X.; Xiong, X.; Zhang, F.; Zheng, H.; Li, D. pH-Responsive nanoparticles based on covalently grafted conjugates of carboxymethyl chitosan and daunorubicin for the delivery of anti-cancer drugs. *J. Biomed. Nanotechnol.* **2017**, *13* (12), 1647−1659.
(37) Abedian, Z.; Jenabian, N.; Moghadamnia, A. A.; Zabihi, E.; Pourbagher, R.; Rajabnia, M. Antibacterial activity of high-molecular-weight and low-molecular-weight chitosan upon oral pathogens. *Int. J. Infect. Dis.* **2020**, *101*, 46−47.
(38) Agrawal, P.; Singh, R. P.; Sharma, G.; Mehata, A. K.; Singh, S.; Rajesh, C. V.; Pandey, B. L.; Koch, B.; Muthu, M. S. Bioadhesive micelles of d-α-tocopherol polyethylene glycol succinate 1000: Synergism of chitosan and transferrin in targeted drug delivery. *Colloids Surf., B* **2017**, *152*, 277−288.
(39) Jalvandi, J.; White, M.; Gao, Y.; Truong, Y. B.; Padhye, R.; Kyratzis, I. L. Polyvinyl alcohol composite nanofibres containing conjugated levofloxacin-chitosan for controlled drug release. *Mater. Sci. Eng.: C* **2017**, *73*, 440−446.
(40) Guo, X. L.; Kang, X. X.; Wang, Y. Q.; Zhang, X. J.; Li, C. J.; Liu, Y.; Du, L. B. Co-delivery of cisplatin and doxorubicin by covalently conjugating with polyamidoamine dendrimer for enhanced synergistic cancer therapy. *Acta Biomater.* **2019**, *84*, 367−377.
(41) Wei, X.; Liao, J.; Davoudi, Z.; Zheng, H.; Chen, J.; Li, D.; Xiong, X.; Yin, Y.; Yu, X.; Xiong, J.; Wang, Q. Folate receptor-targeted and GSH-responsive carboxymethyl chitosan nanoparticles containing covalently entrapped 6-mercaptopurine for enhanced intracellular drug delivery in leukemia. *Mar. Drugs* **2018**, *16* (11), No. 439.
(42) Xu, M.; Asghar, S.; Dai, S.; Wang, Y.; Feng, S.; Jin, L.; Shao, F.; Xiao, Y. Mesenchymal stem cells-curcumin loaded chitosan nanoparticles hybrid vectors for tumor-tropic therapy. *Int. J. Biol. Macromol.* **2019**, *134*, 1002−1012.
(43) Sutar, Y. B.; Telvekar, Y. N. Chitosan based copolymer-drug conjugate and its protein targeted polyelectrolyte complex nanoparticles to enhance the efficiency and specificity of low potency anticancer agent. *Mater. Sci. Eng.: C* **2018**, *92*, 393−406.
(44) Wang, Y.; Yu, H.; Wang, S.; Gai, C.; Cui, X.; Xu, Z.; Li, W.; Zhang, W. Targeted delivery of quercetin by nanoparticles based on chitosan sensitizing paclitaxel-resistant lung cancer cells to paclitaxel. *Mater. Sci. Eng.: C* **2021**, *119*, No. 111442.
(45) Yang, H.; Tang, C.; Yin, C. Estrone-modified pH-sensitive glycol chitosan nanoparticles for drug delivery in breast cancer. *Acta Biomater.* **2018**, *73*, 400−411.
(46) Godse, R.; Rathod, M.; De, A.; Shinde, U. Intravitreal galactose conjugated polymeric nanoparticles of etoposide for retinoblastoma. *J. Drug Delivery Sci. Technol.* **2021**, *61*, No. 102259.
(47) Qu, D.; Jiao, M.; Lin, H.; Tian, C.; Qu, G.; Xue, J.; Xue, L.; Ju, C.; Zhang, C. Anisamide-functionalized pH-responsive amphiphilic chitosan-based paclitaxel micelles for sigma-1 receptor targeted prostate cancer treatment. *Carbohydr. Polym.* **2020**, *229*, No. 115498.
(48) Dutta, B.; Barick, K. C.; Hassan, P. A. Recent advances in active targeting of nanomaterials for anticancer drug delivery. *Adv. Colloid Interface Sci.* **2021**, *296*, No. 102509.
(49) Rostami, E. Progresses in targeted drug delivery systems using chitosan nanoparticles in cancer therapy: A mini-review. *J. Drug Delivery Sci. Technol.* **2020**, *58*, No. 101813.
(50) Wen, P.; Ke, W.; Dirisala, A.; Toh, K.; Tanaka, M.; Li, J. Stealth and pseudo-stealth nanocarriers. *Adv. Drug Delivery Rev.* **2023**, *198*, No. 114895.
(51) Li, L.; Liang, N.; Wang, D.; Yan, P.; Kawashima, Y.; Cui, F.; Sun, S. Amphiphilic polymeric micelles based on deoxycholic acid and folic acid modified chitosan for the delivery of paclitaxel. *Int. J. Mol. Sci.* **2018**, *19* (10), No. 3132.
(52) Bonferoni, M. C.; Sandri, G.; Dellera, E.; Rossi, S.; Ferrari, F.; Mori, M.; Caramella, C. Ionic polymeric micelles based on chitosan and fatty acids and intended for wound healing. Comparison of linoleic and oleic acid. *Eur. J. Pharm. Biopharm.* **2014**, *87* (1), 101−106.
(53) Elsabee, M. Z.; Morsi, R. E.; Fathy, M.Chemical Modifications of Chitin and Chitosan. In *Encyclopedia of Marine Biotechnology*; Wiley, 2020; Vol. 2, pp 885−963.
(54) Chitosan and Its Derivatives as Self-Assembled Systems for Drug Delivery. In *Controlled Drug Delivery*; Mateescu, M. A.; Ispas-Szabo, P.; Assaad, E., Eds.; Woodhead Publishing Limited: Cambridge, U.K., 2015; pp 85−125.
(55) Rippon, J. A.; Evans, D. J. Improving the Properties of Natural Fibres by Chemical Treatments. In *Handbook of Natural Fibres*; Woodhead Publishing, 2020; pp 245−321.
(56) Vasile, C.; Pamfil, D.; Stoleru, E.; Baican, M. New developments in medical applications of hybrid hydrogels containing natural polymers. *Molecules* **2020**, *25* (7), No. 1539.
(57) Junttila, M. R.; Sauvage, F.J.d. Influence of tumour microenvironment heterogeneity on therapeutic response. *Nature* **2013**, *501* (7467), 346−354.
(58) Xin, Z.; Hou, J.; Ding, J.; Yang, Z.; Yan, S.; Liu, C. Surface functionalization of polyethylene via covalent immobilization of O-stearoyl-chitosan. *Appl. Surf. Sci.* **2013**, *279*, 424−431.
(59) Hirano, S.; Ohe, Y.; Ono, H. Selective N-acylation of chitosan. *Carbohydr. Res.* **1976**, *47* (2), 315−320.
(60) Krasnou, I.; Gårdebjer, S.; Tarasova, E.; Larsson, A.; Westman, G.; Krumme, A. Permeability of water and oleic acid in composite films of phase separated polypropylene and cellulose stearate blends. *Carbohydr. Polym.* **2016**, *152*, 450−458.
(61) Nawaz, A.; Wong, T. W. Quantitative characterization of chitosan in the skin by Fourier-transform infrared spectroscopic imaging and ninhydrin assay: application in transdermal sciences. *J. Microsc.* **2016**, *263* (1), 34−42.
(62) Al-Azi, S. O. S. M.; Tan, Y. T. F.; Wong, T. W. Transforming large molecular weight pectin and chitosan into oral protein drug nanoparticulate carrier. *React. Funct. Polym.* **2014**, *84*, 45−52.
(63) El Knidri, H.; El Khalfaouy, R.; Laajeb, A.; Addaou, A.; Lahsini, A. Eco-friendly extraction and characterization of chitin and chitosan from the shrimp shell waste via microwave irradiation. *Process Saf. Environ. Prot.* **2016**, *104* (104), 395−405.
(64) Kumari, S.; Rath, P.; Kumar, A. S. H.; Tiwari, T. N. Extraction and characterization of chitin and chitosan from fishery waste by chemical method. *Environ. Technol. Innovations* **2015**, *3*, 77−85.
(65) Weißpflog, J.; Vehlow, D.; Müller, M.; Kohn, B.; Scheler, U.; Boye, S.; Schwarz, S. Characterization of chitosan with different degree of deacetylation and equal viscosity in dissolved and solid state−Insights by various complimentary methods. *Int. J. Biol. Macromol.* **2021**, *28* (171), 242−261.
(66) Hirai, A.; Odani, H.; Nakajima, A. Determination of degree of deacetylation of chitosan by ^{1}H NMR spectroscopy. *Polym. Bull.* **1991**, *26*, 87−94.
(67) Shi, Y.; Liu, S. A.; Kerwood, D. J.; Goodisman, J.; Dabrowiak, J. C. Pt (IV) complexes as prodrugs for cisplatin. *J. Inorg. Biochem.* **2012**, *107* (1), 6−14.

https://doi.org/10.1021/acsomega.4c03529
ACS Omega 2025, 10, 2428−2441